Proceedings of the ASME 2010 3rd Joint US-European Fluids Engineering Summer Meeting and 8th International Conference on Nanochannels, Microchannels, and Minichannels
FEDSM-ICNMM2010
August 1-5, 2010, Montreal, Canada

FEDSM-ICNMM2010-30989

HEAT AND MASS TRANSFER IN THE CORNER FLOW REGION OF VERTICAL MICROGROOVES

Xuelei Nie[a, b]
[a]Institute of Engineering Thermophysics, CAS
Beijing, China
[b]School of Mechanical Engineering
Purdue University, West Lafayette, IN, USA

Xuegong Hu*
Institute of Engineering Thermophysics, CAS
Beijing, China
xuegonghu@mail.etp.ac.cn

Suresh V. Garimella
School of Mechanical Engineering
Purdue University, West Lafayette, IN, USA

Dawei Tang
Institute of Engineering Thermophysics, CAS
Beijing, China

ABSTRACT

Evaporation of the thin film formed in microgrooves is associated with high heat transfer rates. One of the factors that limits this heat transfer is the capacity of the microgroove to drive fluid into the thin film. The mass flow rate and mass flux in the corner flow region of a microgroove is experimentally and theoretically investigated in this work. The experiments yield the speed at which wetting occurs in vertical microgrooves. The wetting speed reflects the balance between the gravitational, viscous and capillary forces acting on the film. A force balance is also conducted on the liquid in the corner flow region of the microgrooves. This analysis allows a calculation of the maximum amount of liquid that the microgrooves can drive to the evaporating surface in the corner flow region, which in turn determines the maximum evaporation rate in this localized area.

*Corresponding Author

1 INTRODUCTION

Significant research attention has been focused on transport in microgrooves due to their capacity for supporting high heat transfer rates. Microgrooves are used as wicks in the evaporator region of heat pipes, capillary pumped loops (CPL) and other phase-change heat transfer systems. Evaporation in the thin films formed in the microgrooves contributes to high heat transfer rates in these structures. While thin films have been widely studied, analytical treatment of the mass flow rate in microgrooves has received less attention. Wang et al. [1] developed a model based on augmented Young-Laplace equation to predict the total heat transfer in thin-film region. Dhavaleswarapu et al. [2] used the micro-PIV (particle image velocimetry) to observe the fluid flow in an evaporating meniscus. Do et al. [3] developed a mathematical model to study the evaporation and condensation on meniscus in groove wick.

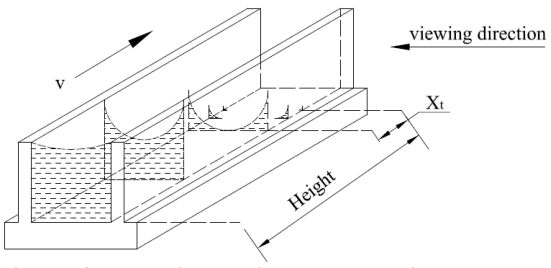

FIG. 1 LIQUID FLOW PROFILE DEVELOPMENT IN A RECTANGULAR MICROGROOVE.

A vertical plate with microgrooves immersed one end in a liquid reservoir draws liquid into the microgrooves due to the axial gradient in capillary pressure. According to the work of Nilson and Tchikanda [4], the liquid film in a microgroove can be divided into three regions along the axis of the microgroove – an entry region where the meniscus is attached to the top corner of the channel, a jump-like transition region, and a corner flow region where the meniscus recedes into the two bottom corners of the rectangular microgroove. The thin liquid films in the corner flow region experience more intensive evaporation than the other regions. In turn, the evaporation in the corner flow region is affected by the fluid mass flow rate that can be driven into this region. The small size of the liquid film in this region makes direct measurements of mass flow rate difficult. In the present work, a combined experimental and theoretical analysis is employed to explore the fluid mass flow rate in the corner flow region of microgrooves.

2 EXPERIMENTAL APPROACH

A number of past studies have used theoretical and experimental methods to predict wetting length, fluid flow and heat transfer in triangular microgrooves [5,6,7]. The corner flow region in rectangular microgrooves can be considered to be similar to that in triangular microgrooves as illustrated in Fig. 2. Hence an approach similar to that of Catton and Stroes [7] is adopted for the present analysis.

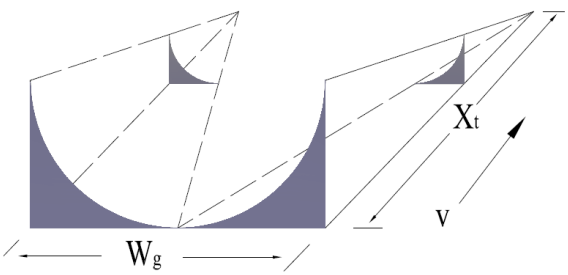

FIG. 2 CORNER FLOW REGION.

Experiments were first conducted to determine the wetting speed of the working fluids on a vertical copper plate with rectangular microgrooves, when one end of the plate is immersed in a reservoir of the liquid. A high speed camera is employed to visualize the wetting process (as shown in Fig. 3b). The wetted height in the microgrooves above the reservoir surface is measured as a function of time with the help of a ruler attached in the field of view to the copper plate. Thus, the wetting speed at different heights along the microgroove is determined.

Fig. 3a shows a sketch of this experimental setup to determine wetting speed. The working fluids are distilled water and ethanol. The size of the copper plate is 20 mm × 110 mm × 3 mm, and the microgrooves are fabricated on the plate with wire EDM. The microgrooves are of width 0.2 mm and depth 0.8 mm, with a groove pitch of 0.4 mm, and extend the full 110 mm length of the plate. Images are captured with a high-speed camera (Phantom 5.0 from Vision Research) captures images at 200 fps with an exposure time for each frame of 300 µs.

Due to the sensitivity of the wetting process to the quality of the copper surface, a two-step cleaning procedure is used. The copper plate is first cleaned in an ultrasonic bath with a soap solution for 60 minutes. The soap solution is then replaced in the bath with distilled water and the plate is cleaned for another 30 minutes, and then air-dried. Once the plate is mounted vertically in the reservoir the camera is triggered just prior to the addition of 5 ml of liquid to the reservoir. The visualization continues until the height of the liquid in the microgrooves no longer increases.

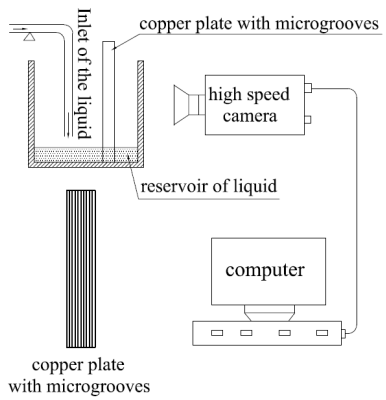

(a)

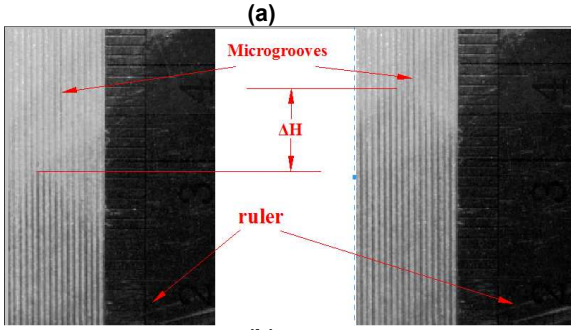

(b)

FIG. 3 (a) EXPERIMENTAL APPROACH FOR MEASURING THE WETTING SPEED, AND (b) SAMPLE IMAGES AT DIFFERENT TIMES IN THE WETTING PROCESS.

3 THEORETICAL APPROACH

The mass flux in the corner flow region is determined through a theoretical analysis which uses the wetting speed determined in the experiments as an input.

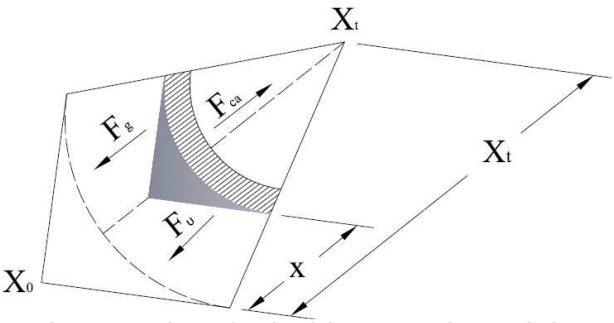

FIG. 4 PART SKETCH OF CORNER FLOW REGION.

The following assumptions are made in the analysis:

(1) As shown in Fig. 4 and 5, the film thickness h, measured from the corner to the liquid-air interface, decreases along the axial direction from X_0 to X_t. Based on analysis and experiments, Stroes [8] suggested that this variation h(x) takes the form:

$$h(x) = ax^2 + bx + c \qquad (1)$$

Here, a, b and c are constants for a given microgroove and working liquid, x is the distance away from the origin X_0 along the axial direction of the microgroove. In addition, the shape of the meniscus in this region is assumed to be circular, with radius r (as shown in Fig. 5), as is common in the literature.

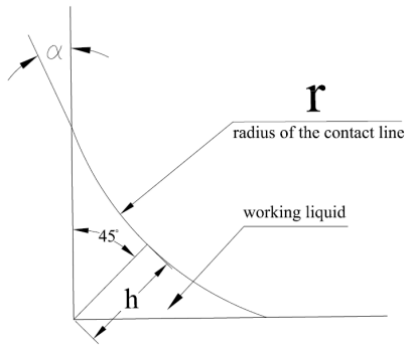

FIG. 5 CROSS SECTION OF THE CORNER FLOW REGION.

(2) Experimentally captured meniscus shapes for water and ethanol are shown in Fig. 6 [9]. It is clear from these images that the transition from the corner flow region to the dry region along the bottom of the microgroove is nearly flat; hence, it is reasonable to assume a value of zero for the "apparent" contact angle at this location.

(3) All the liquid in this region is assumed to evaporate, with no boiling occurring.

(4) Since the sensible heating of the liquid is much smaller than its latent heat, sensible heating is ignored in this analysis.

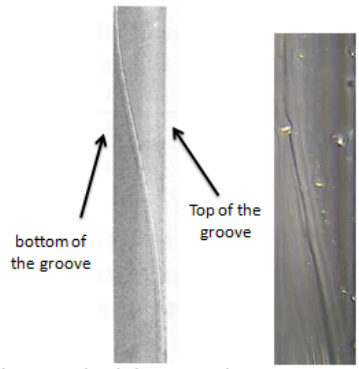

FIG. 6 PHOTOGRAPH OF THE MENISCUS SHOWING THE CONTACT LINE BETWEEN LIQUID AND AIR IN SIDE VIEW. THE IMAGE ON THE LEFT IS FOR DISTILLED WATER, WHILE THAT ON THE RIGHT IS FOR ETHANOL.

Evaporation of liquid in the corner flow region is compensated by liquid entering this region from the other two regions. At a height H above the reservoir liquid level, the velocity of liquid entering the corner flow region, averaged over the corner flow cross section, is assumed to be equal to half of the wetting speed at the same height because the measured wetting speed reflects the velocity at the free surface of the film, which is higher than that in the bulk of the film. Since the average velocity at which the microgroove compensates for the liquid loss in the corner flow region is equal to half of the wetting speed at this height, the mass flow rate in the corner flow region can be calculated. If the average cross-sectional area of the corner flow region S_{acs} can be calculated (as will be described in the following), the mass flow rate entering the corner flow region can be written as

$$m = S_{acs} v \rho / 2$$

A force balance on the liquid in the corner flow region provides the average cross-sectional area of this region, as described next.

A thin cross-sectional slice of liquid in the corner flow region is considered as shown in Fig. 4 (shown as the shaded region). The force balance on this liquid slice gives

$$F_{ch} = F_\upsilon + F_g \qquad (2)$$

Here, F_{ch} is the capillary head, which is the capillary pressure gradient in the liquid caused by the changing curvature of the liquid-air interface in the microgroove. F_υ is the viscous force exerted by the microgroove wall to oppose the motion of the working fluid. F_g is the gravitional force. Following [7], the three force terms F_{ch}, F_υ and F_g may be written as:

$$F_{ch} = -\frac{dP_l}{dx} = \frac{d}{dx}\left(\frac{\sigma}{r(x)}\right) = -\frac{\sigma}{r(x)^2}\frac{dr}{dx} \quad (3)$$

$$F_g = \rho g \quad (4)$$

$$F_\upsilon = \frac{Km(x)\upsilon_l}{2S(x)D(x)^2} \quad (5)$$

In Eq. (3) and (4), r(x) is the radius of the interface, σ is the surface tension of the liquid, P_l is the liquid pressure, ρ is the density of liquid and g is the gravitational acceleration. In Eq. (5), υ_l is kinematic viscosity of the liquid, D(x) is the hydraulic diameter of the cross section, S(x) is the liquid cross-sectional area in one corner flow region (i.e., in one triangular region, and half of the total flow cross-section), m(x) is half of the liquid mass flow rate at x, and K is the friction factor. Ayyaswamy et al. [10] recommend values for K of 33.993 and 52.0861 respectively for a triangular groove with a half-angle of 45 degree and liquid contact angles of zero (ethanol) and 28 deg. (water).

From the geometrical sketch of the crosssection in the corner flow region shown in Fig. 5 and the definitions of S(x), and D(x), the following expressions can be written:

$$S(x) = [r(x)cos\alpha]^2 - r(x)^2 sin\alpha \cos\alpha - \frac{1}{2}r(x)^2(\frac{\pi}{2} - 2\alpha) \quad (6)$$

$$D(x) = \frac{S(x)}{r(x)(cos\alpha - sin\alpha)} \quad (7)$$

Per assumption (3) above, the evaporative mass flow rate may be written as:

$$m(x) = \frac{w_g}{2h_{fg}}\int_x^{X_t} q(x)dx \quad (8)$$

in which q(x) is the heat flux imposed on the wall, W_g is the width of the microgroove, and h_{fg} is the latent heat of the liquid. Stroes [8] gave the following expression for the heat flux distribution along the axial direction of the groove in the corner flow region:

$$q(x) = 3q_0(\frac{x}{X_t})^2 \quad (9)$$

where q_0 is the average heat flux imposed on the corner flow region. Substituting Eq. (8) and (9) into Eq. (5), the frictional force term F_υ becomes:

$$F_\upsilon = \frac{K\upsilon w_g q_0}{4S(x)D(x)^2 h_{fg} X_t^2}(X_t^3 - x^3) \quad (10)$$

Substituting Eq. (3), (4), (10) into Eq. (2), the force balance for a liquid slice in the corner flow region can be expressed as

$$\frac{dr}{dx} = -\frac{K\upsilon w_g q_0 r(x)^2}{4S(x)D(x)^2 h_{fg} X_t^2 \sigma}\left(X_t^3 - x^3\right) - \frac{\rho g}{\sigma}r(x)^2 \quad (11)$$

Integrating Eq. (11) from X_0 to X_t in the corner flow region,

$$\int_{r_0}^{r_{min}} dr = -\int_{X_0}^{X_t}\frac{K\upsilon w_g q_0 r(x)^2}{4S(x)D(x)^2 h_{fg} X_t^2 \sigma}\left(X_t^3 - x^3\right)dx - \int_{X_0}^{X_t}\frac{\rho g}{\sigma}r(x)^2 dx \quad (12)$$

From the geometrical sketch in Fig. 5, the following relation between r(x) and h(x) is derived:

$$h(x) = r(x)(\frac{1}{sin45^\circ} - \frac{1-cos\alpha}{sin45^\circ} - 1) \quad (13)$$

in which α is the contact angle (0 deg. and 28 deg. [11] for ethanol and water, respectively). Based on assumptions (1) and (2), h(x) is known. The boundary conditions for calculating the constants a, b and c are shown as follows:

$$h(x_0) = h(0) = \frac{w_g}{2(cos\alpha - sin\alpha)}(\frac{1}{sin45^\circ} - \frac{1-cos\alpha}{sin45^\circ} - 1)$$

$$h(x_t) = r_{min}(\frac{1}{sin45^\circ} - 1)$$

$$\frac{dh}{dx}|_{X_t} = 2aX_t + b = 0$$

where r_{min} is the minimum corner radius of the microgroove. Eq. (1) and (13) are substituted into Eq. (12) and the equation is integrated. Since the value of q_0 in this equation is unknown, a small initial value is given (which is iterated upon as described below), which leaves only X_t as the unknown. Solving the new equation yields the value of X_t, which represents the length of the corner flow region.

From Eq. (1), (6), (13) and X_t, the average cross-sectional area of the corner flow region S_{acs} may be determined through the following integration:

$$S_{acs} = \frac{\int_0^{X_t} S(x)dx}{X_t} \quad (14)$$

The mass flow rate and the average mass flux in the corner flow region are then obtained as

$$m(X_0) = S_{acs}\upsilon\rho/2 \quad (15)$$

$$M = \frac{S_{acs}\upsilon\rho}{2W_g X_t} \quad (16)$$

Based on the mass flux from Eq. (16), the average heat flux q_0 imposed can be obtained as

$$q_0 = Mh_{fg} \quad (17)$$

The average heat flux q_0 calculated with the Eq. (17) would differ from the initial value assumed above for q_0. Iteration with

new initial values of q_0 in Eq. (9) until the q_0 calculated with Eq. (17) is equal to the initial guess provides the final correct value of X_t.

4 RESULTS AND DISCUSSION

The experimentally determined wetting speed in the rectangular microgrooves is plotted in Fig. 7 as a function of height above the reservoir surface. The results show that the wetting speed is high at the beginning, as soon as the plate is immersed in the liquid, and then decreases with time. After a period of time, the length of the wetted microgrooves reaches a final value and the wetting speed decreases to zero. The final length of the wetted microgrooves with distilled water as the working fluid is longer than that with ethanol because the surface tension of distilled water is larger.

These experimental results for wetting speed driven by the capillary head in the corner flow region are used as an input in the analytical model.

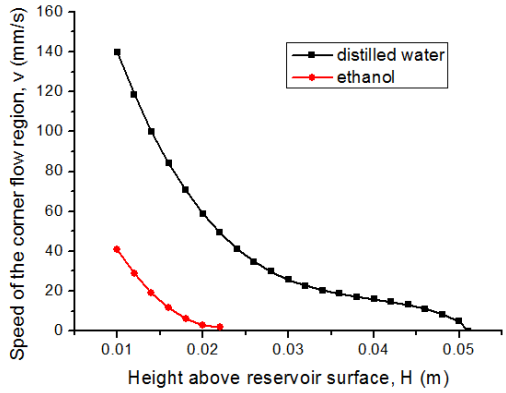

FIG. 7 EXPERIMENTAL RESULTS FOR THE WETTING SPEED IN THE CORNER FLOW REGION AS A FUNCTION OF HEIGHT ABOVE THE RESERVOIR.

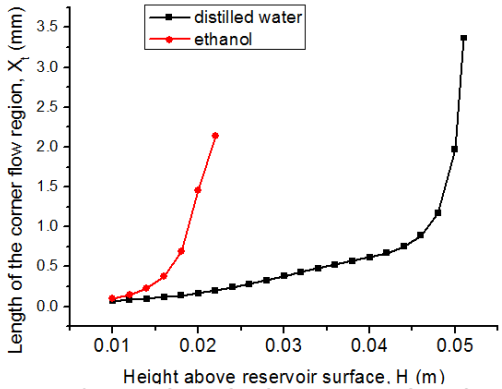

FIG. 8 ANALYTICAL RESULTS FOR THE LENGTH OF THE CORNER FLOW REGION AS A FUNCTION OF HEIGHT ABOVE THE RESERVOIR.

Fig. 8 shows the length of the corner flow region X_t as a function of height during the wetting process, calculated through the force balance described earlier. The length of the corner flow region increases with height above the reservoir, with the length being greater with distilled water than with ethanol for a given height. Based on this result and assumption (1) above, the shape and size of the corner flow region can be obtained.

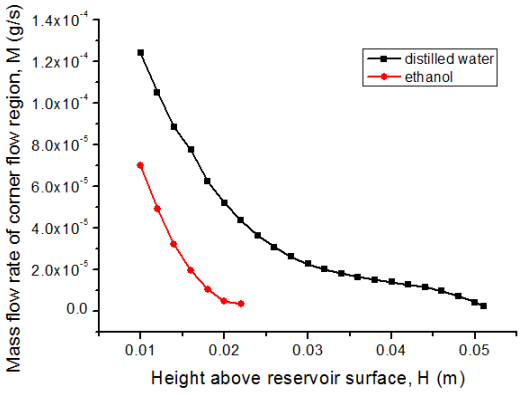

FIG. 9 ANALYTICAL RESULTS FOR MASS FLOW RATE OF LIQUID IN CORNER FLOW REGION AS A FUNCTION OF HEIGHT ABOVE THE RESERVOIR.

Fig. 9 and 10 show results for the mass flow rate and mass flux in the corner flow region. Both quantities decrease as the height above the reservoir increases, commensurate with the decrease in capillary head.

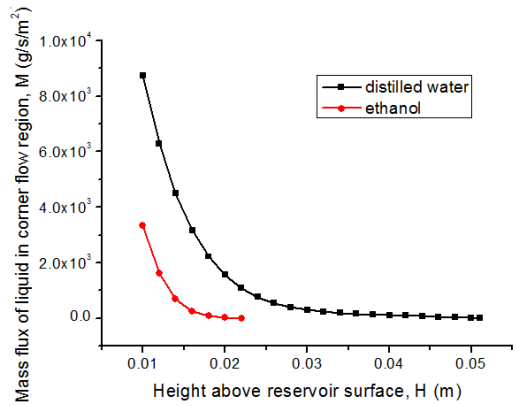

FIG. 10 ANALYTICAL RESULTS FOR AVERAGE MASS FLUX IN CORNER FLOW REGION AS A FUNCTION OF HEIGHT ABOVE THE RESERVOIR.

As all of the liquid driven to the corner flow region evaporates, the heat transfer rate in this region is limited only by the mass flux available as a result of the capillary head. This work thus offers reference values for mass flow rate and mass flux in the corner flow region in vertical microgrooves for distilled water and ethanol as the working fluids.

The maximum possible heat flux in the corner flow region in microgrooves may now be estimated as shown in Fig. 11. These values range from ~2.0×10^7 W/m^2 at a height of 10 mm to 0 at a height of 52 mm for distilled water; corresponding values for ethanol are ~3×10^6 W/m^2 at a height of 10 mm to 0 at a height of 24 mm. While the actual heat flux achieved in the

corner flow region is governed by a number of factors, the values derived here provide the mass flux-limited maxima. With other limiting factors considered, the true maximum heat flux in the corner flow region would be expected to be much smaller than the values shown in Fig. 11.

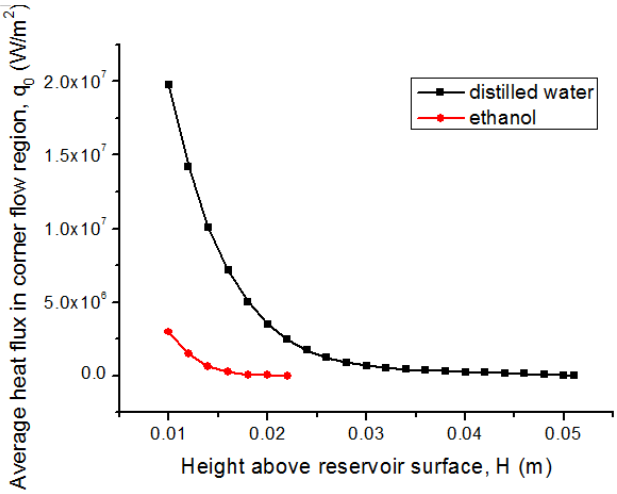

FIG. 11 ANALYTICAL RESULTS FOR THE AVERAGE HEAT FLUX IN CORNER FLOW REGION AS A FUNCTION OF HEIGHT ABOVE RESERVOIR.

5 CONCLUSIONS

The present work helps estimate the shape and size of the liquid film in the corner flow region, and the fluid flow and heat transfer in this region as the microgrooves are wetted, based on experimentally measured wetting speeds. The following conlusions may be drawn based on these results:

(1) During the wetting process of vertical microgrooves, the wetting speed decreases sharply as the wetted length of the microgrooves increases. The wetting speed is much higher with distilled water working fluid than with ethanol for a given wetted length. The wetted length of the microgrooves with distilled water working fluid is two times the length with ethanol working fluid.

(2) The length of the corner flow region in microgrooves increases as the wetted length increases, but the mass flow rate, mass flux and the possible maximum heat flux in the corner flow region correspondingly decrease. For distilled water, working fluid mass flux and heat flux values are 8745 g/(s·m^2) and 2.0×10^7 W/m^2 respectively at a height of 10 mm; by a height of 52 mm, they drop to zero. Corresponding values for ethanol working fluid are 3330 g/(s·m^2) and 3×10^6 W/m^2 at a height of 10 mm, and drop to zero at a height of 24 mm.

ACKNOWLEDGMENTS

The authors acknowledge the financial support provided by National Natural Science Foundation of China (Grant No. 50776088).

REFERENCES

[1] H. Wang, S. V. Garimella, An analytical solution for the total heat transfer in the thin-film region of an evaporating meniscus, Int. J. Heat Mass Transfer 51 (2008) 6317 — 6322.

[2] H. K. Dhavaleswarapu, P. Chamarthy, Experimental investigation of steady buoyant-thermocapillary convection near an evaporating meniscus, Physics of Fluids 19 082103 (2007).

[3] K. H. Do, S. J. Kim, A mathematical model for analyzing the thermal characteristics of a flat micro heat pipe with a grooved wick, Int. J. Heat Mass Transfer 51 (2008) 4637 — 4650.

[4] R. H. Nilson, S. W. Tchikanda, Steady evaporating flow in rectangular microchannels, Int. J. Heat Mass Transfer 50 (2007) 3933 — 3942.

[5] X. Xu, V. P. Carey, Film evaporation from a micro-grooved surface — an approximate heat transfer model and its comparison with experimental data, J. Thermophysics 4 (1990) 512 — 520.

[6] J. M. Ha, G. P. peterson, Analytical prediction of the axial dryout point for evaporating liquids in triangular microgrooves, J Heat Transfer, 116 (1994) 498 — 503.

[7] I. Catton, . G. R. Stroes, A semi-analytical model to predict the capillary limit of heated inclined triangular capillary grooves, J. Heat Transfer, 124 (2002) 162 — 168.

[8] G. R. Stroes, An experimental and analytical investigation of the wetted length supported in inclined capillary grooves heated from below, PhD thesis, UCLA, Los Angeles, CA., 1997.

[9] T. Wang, X. G. Hu, D. W. Tang, Study on the characteristic of contact line in a triangle-wetting region of rectangular capillary microgrooves, Journal of Engineering Thermophysics, 2009, (11).

[10] P. S. Ayyaswamy, I. Catton, D. K. Edwards, Capillary flow in triangular grooves, J. Applied Mechanics, 41 (1974) 332 — 336.

[11] A. Horsthemke, J. J. Schroder, The wettability of industrial surfaces: contact angle measurements and thermodynamic analysis, Chem. Eng. Fundam., 2 (1983) 66 — 74.